Zwitterionic Silenes: Interesting Goals for Synthesis?

Henrik Ottosson*[a]

Abstract: Properties of silenes, as a function of increased reversal of the Si=C bond polarity, have been examined through quantum-chemical calculations. The aim of this study was to identify silenes that can be of general interest for organic synthesis. The calculations were carried out primarily with the B3LYP hybrid density functional method, but also with the CASSCF, MP2, MP4(SDQ), and CCSD(T) methods. The study was performed on $Z_2Si{=}CXY$ compounds which were divided into three sets that differ with regard to their Si substituents (Z), and with their C substituents (X and Y) varying from weakly to strongly π-electron-donating groups. The charge at the Si atom (q(Si)) was used as a measure of the extent of reversed silicon–carbon bond polarity. For each of the three sets, the variation in silicon–carbon bond lengths ($r_{Si=C}$) and extent of Si pyramidalization (ΣSi) in relation to q(Si) follow three separate curves. Silenes with strongly π-electron-donating X and Y groups are completely described by zwitterionic (reverse-polarized) resonance structures. Such zwitterionic silenes are singly (Si−C) rather than doubly bonded (Si=C), and have a distinctly pyramidal Si atom due to negative charge localization. These silenes also have much lower heats of dimerization than the parent silene. Finally, inversion barriers of zwitterionic silenes are increased by electron-withdrawing substituents, and this enables computational design of silenes with their Si atoms as chiral centers. It is hoped that such chiral zwitterionic silenes can find use in organic synthesis.

Keywords: electronic structure · reversed polarization · silenes · silicon · zwitterions

Introduction

Silenes (i.e., compounds with Si=C bonds) are highly labile at ambient conditions and in contrast to alkenes they often dimerize in the absence of reaction partners.[1] Apeloig and Karni demonstrated that kinetic stabilization of such species is obtained by lowering their Si=C bond dipole moments through electron delocalization from π electron-donating groups,[2] and the first stable and solid silene, 1,1-bis(trimethylsilyl)-2-(trimethylsiloxy)-2-(1-adamantyl)-1-silaethene, generated by Brook and co-workers,[3] is an elegant example in which this type of stabilization is operative (Scheme 1). In this silene, a zwitterionic resonance structure of type **II** contributes to the electronic structure and leads to a smaller Si=C bond dipole; the term reversed polarity was coined for the π conjugative effect that reduces the natural $Si^{\delta+}{=}C^{\delta-}$ polarization.[2] Indeed, Apeloig and Karni found through ab initio calculations at the Hartree–Fock level that "reversed polarity of the π bond (i.e., $Si^{\delta-}{=}C^{\delta+}$) is the most important single electronic factor that reduces the reactivity of silenes; the energies of π and π* orbitals are less significant".[2] In a series of laser flash photolytic studies, Leigh and co-workers probed the reactivities of transient silenes substituted at either the Si or C atom toward MeOH.[4] They found that π-donor/σ-acceptor substituents at Si enhance the electrophilicity of the Si=C bond, whereas π-acceptor/σ-donor substituents at Si and π-donor substituents at C have the opposite effect. This verifies that the silicon–carbon bond polarity is the main factor affecting the reactivity of silenes.

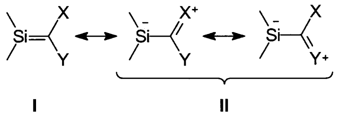

Scheme 1. Possible resonance structures of a silene with π electron-donating substituents on the carbon atom.

However, is there a limit to the contribution of a zwitterionic resonance structure of type **II**, or are there silenes for which it fully describes the electronic structure?

---

[a] Dr. H. Ottosson
Department of Organic Chemistry, Institute of Chemistry
Box 599, Uppsala University, 751 24 Uppsala (Sweden)
Fax: (+46) 18-471-3818
E-mail: Henrik.Ottosson@kemi.uu.se

Supporting information for this article is available on the WWW under http://www.chemeurj.org or from the author: Three tables with symmetries, absolute and relative energies, atomic charge at Si, $r_{Si=C}$, ΣSi of the silenes, and ΣE_{ST} of silylenes and carbenes. Cartesian coordinates of the 184 different silene conformers are available upon request from the author.

DOI: 10.1002/chem.200204583

In the latter case, the formal Si=C double bond will transform into a Si–C single bond, and the Si atom should resemble the Si of a silyl anion. Silenes in which there is lowered or reversed silicon–carbon bond polarity will also have reduced tendencies to form the dipole–dipole complexes that should precede dimerization. Such silenes would thus be stabilized kinetically toward dimerization, but what about their thermodynamic stability?

Among the Si=C bonded compounds that have been studied so far, the silene reported by Brook and co-workers,[3] the 4-silatriafulvenes reported by Kira and co-workers,[5] the 1-silaallenes of West and co-workers,[6] and our 1,1-bis(trimethylsilyl)-2-amino-2-siloxysilenes[7] have lower Si=C bond polarities than the parent silene. In this regard, 2-silenolates[8, 9] are also interesting, since these systems can have a negative charge localized to Si, and depending on the extent of charge localization they may be designated as $Si^{\delta-}=C^{\delta+}$ polarized silenes. Indeed, our recent X-ray crystal structure of 1-*t*Bu-2,2-bis(trimethylsilyl)-2-silenolate revealed that this 2-silenolate is Si–C singly bonded,[9] proving that they are strongly affected by reversed polarization. The silaketene H_2SiCO studied by Maier and co-workers[10] and the [1,2-$C_6H_4[N(R)]_2C$–$Si[N(R)]_2C_6H_4$-1,2 (R = CH_2tBu)] silylene–carbene complex of Lappert and co-workers[11] should also be noted, since these formally could be written as Si=C bonded; however, in reality these compounds are donor–acceptor complexes with the utmost weak silicon–carbon bonds.

In neutral silenes and 1-silaallenes with reduced silicon–carbon bond polarities, silicon–carbon bond distances within 1.693–1.917 Å were either observed or calculated.[3, 5–7] In the parent 2-silenolate a silicon–carbon distance of 1.926 Å was calculated at the HF/6-31G(d) level,[8] and in our recent crystal structure of 1-*t*Bu-2,2-bis(trimethylsilyl)-2-silenolate an Si–C bond with the same length was measured.[9] In Lappert's silylene–carbene complex a distance as long as 2.162 Å was observed.[11] The extended silicon–carbon bonds in these compounds are contrasted by the silicon–carbon distances of 1.7039 and 1.692 Å for $H_2Si=CH_2$ and $Me_2Si=CH_2$ measured by millimeter and microwave spectroscopy,[12, 13] and the silicon–carbon distances of 1.702–1.741 Å in the aryl-, alkyl-, and/or silyl-substituted silenes reported by Apeloig et al. and Wiberg et al.[14, 15] Moreover, Si pyramidalizations were calculated for the parent 2-silenolate,[8] variously substituted 4-silatriafulvenes,[5] and in 1,1-bis(trimethylsilyl)-2-amino-2-siloxysilenes[7] and observed in our recent 2-silenolate,[9] in H_2SiCO,[10] and in the [1,2-$C_6H_4[N(R)]_2C$–$Si[N(R)]_2C_6H_4$-1,2 (R = CH_2tBu)] complex.[11] It was also concluded that negative charge in the silylene–carbene complex is located at Si,[11] and its long silicon–carbon bond can be rationalized by very extensive reversed polarization. Bonding situations intermediate between those of a double-bonded silene and the silylene–carbene complex are easy to envision.

The bonding and electronic structure of heavy alkenes has attracted considerable attention throughout recent decades. Carter and Goddard,[16] as well as Malrieu and Trinquier (in the so-called CGMT theory),[17] connected the bond strength and deviation from planarity of double-bonded $X_2A=BY_2$ compounds to the sum of the singlet–triplet energy splitting ($\Sigma\Delta E_{ST}$) of the X_2A: and Y_2B: fragments.[18] It was shown that heavy alkenes with X and Y as π donor groups have nonclassical *trans*-bent structures with pyramidal A and B atoms when the two interacting fragments have singlet ground states and when Equation (1) is valid.

$$\Sigma\Delta E_{ST} \geq \tfrac{1}{2}E_{\sigma+\pi}[1+(q_1+q_2)/2]+\alpha q_1 q_2 = f(E_{\sigma+\pi}) \qquad (1)$$

In this formula, α is a proportionality factor set to 200 kcal mol^{-1}, q_1 and q_2 are the partial charges of the pπ orbitals of the AX_2 and BY_2 fragments, and $E_{\sigma+\pi}$ is the total A=B bond energy.[17a] The CGMT theory was applied by Karni and Apeloig, and later by Chen, Su, and Chu when exploring the geometries of disilenes, digermenes, and germasilenes,[19, 20] and it was found that the double bond lengths, the tendency toward *trans* bending, and the bond dissociation energies correlate linearly with $\Sigma\Delta E_{ST}$. Some alternative ways to view the bonding in heavy alkenes were also put forward. Jacobsen and Ziegler showed that the *trans* bending and the bond weakening stem from enhanced interatomic as well as intra-atomic Pauli repulsion,[21] whereas Liang and Allen revealed that geometries of Group 14 A=A double bonds are determined by both their intrinsic π–σ* separation and substituent electronegativity.[22]

Kira and co-workers found a connection between the aromaticity of the three-membered ring in 4-silatriafulvene derivatives and their Si=C bond lengths, but no direct correlation between the ring aromaticity and the extent of Si pyramidalization was revealed.[5] However, increased aromaticity in this system implies increased importance of a resonance structure with a cyclopropenium ring and a negatively charged Si atom (i.e., a zwitterionic type **II** structure). Thus, an alternative way to look at the Si pyramidalizations in silenes influenced by reversed polarization may be found by analogy with silyl anions. The latter are distinctly pyramidal,[23] and an increased contribution of reversed polarization in silenes should lead to successively less positively charged and more pyramidal Si atoms. The theory of reversed polarization may thus also explain Si pyramidalizations, and its connection to the CGMT theory should be sought.

We will now analyze how closely the reversed polarization effect is connected to the geometric structures of formally Si=C bonded species, and how the extent of reversed polarization affects their thermodynamic stability. Moreover, are there additional aspects of silenes strongly influenced by reversed Si=C bond polarization that render them interesting from experimental points of view? For example, can silenes be tailored that have inversion barriers sufficiently high to prevent inversion at temperatures used in organic synthesis? If so, one may computationally design a silene with Si as a chiral center. These and other issues will be analyzed next.

Computational details: Geometry optimizations were carried out at the B3LYP/6-31+G(d) level for all silenes.[24, 25] The characters of the stationary points were checked at the B3LYP/6-31+G(d) level by frequency calculations. Atomic charges were calculated by natural population analysis[26] by using the B3LYP/6-31 + G(d) densities. One silene which is strongly influenced by reversed polarization was also optimized at the CASSCF/6-31 + G(d) level, as well as at MP4(SDQ) and CCSD(T) levels by using the 6-311 + G(2d) basis set of McLean and Chandler for Si,[27] and the 6-311 + G(d,p) basis set for all other atoms.[28] To simulate the action of a polar solvent on the structures of some selected silenes, we used the continuum model (PCM) of Tomasi and co-workers.[29] The nature of the bonding interaction in the silicon–carbon bond was investigated with the help of the calculated electron density distribution $\rho(r_b)$ and the energy density distribution $H(r_b)$ at the bond critical point r_b, as described by Cremer and Kraka.[30] The Gaussian 98 program package was used throughout the study,[31] except for the electron density analysis for which AIM2000 was used.[32]

Results and Discussion

The aim of this study was to probe how a gradually increasing contribution of reversed polarization to the electronic structure of silenes affects their geometric structures and thermodynamic stabilities. For this purpose, three sets of $Z_2Si{=}CXY$ silenes (Scheme 2 and Table 1), differing with regard to the substituent Z, were studied (set **A**: Z = H; set **B**: Z = Me; set **C**: Z = SiH_3). The X and Y groups chosen were the increasingly more π electron-donating substituents H, Cl, SH, F, OH, and NH_2. We also included monoanionic, formally Si=C bonded systems $Z_2Si{=}CXY^-$ with X = H, Cl, SH, F, OH, or NH_2, and $Y^- = S^-$, O^-, or NH^-. A total of 117 formally Si=C bonded compounds, which exist in 184 different conformations, were studied. We refrained from including silenes with Z = NH_2, OH, or F, since these substituents form intramolecular hydrogen bonds with some of the X and Y substituents and this would bias the study on the connection between reversed polarity and geometry. For complete data on individual silenes see the Supporting Information.

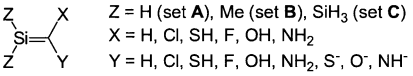

Scheme 2. Investigated compounds.

Table 1. Numbering of investigated compounds.

Y	X: H	Cl	SH	F	OH	NH_2
H	**1**	–	–	–	–	–
Cl	**2**	**3**	–	–	–	–
SH	**4**	**5**	**6**	–	–	–
F	**7**	**8**	**9**	**10**	–	–
OH	**11**	**12**	**13**	**14**	**15**	–
NH_2	**16**	**17**	**18**	**19**	**20**	**21**
S^-	**22**	**23**	**24**	**25**	**26**	**27**
O^-	**28**	**29**	**30**	**31**	**32**	**33**
NH^-	**34**	**35**	**36**	**37**	**38**	**39**

Electronic structure of $Si^{\delta+}{=}C^{\delta-}$ and $Si^{\delta-}{=}C^{\delta+}$ polarized silenes: To investigate the vast number of different silenes, an inexpensive method yielding correct results for all silenes is required. The choice naturally falls on a density functional theory (DFT) method, but it needs to be proven that this method performs well for both naturally ($Si^{\delta+}{=}C^{\delta-}$) and reverse-polarized silenes ($Si^{\delta-}{=}C^{\delta+}$).

For the parent silene **1A** the Si–C distance has been determined as 1.7043 Å at the CCSD(T)/cc-pV(Q,T)Z level,[12] which is in excellent agreement with the value of 1.7039 Å measured by millimeter-wave spectroscopy.[12] The corresponding B3LYP/6-31 + G(d) value is 1.713 Å. For **1B**, the B3LYP/6-31 + G(d) Si–C distance is also 1.713 Å, and the distance found through microwave spectroscopy is 1.692 Å.[13] Thus, B3LYP/6-31 + G(d) gives Si–C distances for naturally polarized silenes that are slightly longer than those measured, but they are well within an acceptable range. As can be expected, the multiconfigurational character of **1A**, as revealed by T_1-diagnostics of the CCSD/6-311 + G(d)//B3LYP/6-31 + G(d) wave function,[33] is low because the norm of the singles amplitude vector (0.015) is below the threshold value for multireference character (0.02).

A T_1-diagnostics of the CCSD/6-311 + G(d)//B3LYP/6-31 + G(d) wave function of $H_2Si{=}C(NH_2)_2$ (**21A**) (i.e., a silene strongly influenced by reversed polarization) gives the norm of the singles amplitude vector as 0.019. Moreover, a CASSCF(10,8)/6-31 + G(d) calculation on **21A**, with the active space including the π(SiC), π*(SiC), the two lp(N), and the four $\sigma(SiH_2)$ and $\sigma^*(SiH_2)$ orbitals, showed that the dominant electron configuration corresponds to the RHF configuration and that it constitutes 96% of the CASSCF wave function. It is thus justified to use single-reference determinant methods for naturally polarized silenes as well as for silenes strongly influenced by reversed polarity. It is not surprising that the CASSCF(10,8)/6-31 + G(d) and HF/6-31 + G(d) geometries of **21A** are similar (CASSCF: $r_{Si=C} = 1.979$ Å and $\Sigma Si = 287.1°$; HF: $r_{Si=C} = 1.983$ Å and $\Sigma Si = 282.9°$).

To obtain benchmark values for geometrical parameters of **21A**, a CCSD(T) optimization was performed with preceding MP2 and MP4(SDQ) optimizations. The CCSD(T)/6-311 + G(2d,d,p) calculation results in $r_{Si=C} = 1.934$ Å and $\Sigma Si = 284.6°$, whereas the values at the MP2/6-311 + G(d,p) and MP4(SDQ)/6-311 + G(2d,d,p) levels are 1.918 Å and 285.4°, and 1.938 Å and 282.7°, respectively. On going to the inexpensive B3LYP/6-31 + G(d) level we obtain $r_{Si=C} = 1.930$ Å and $\Sigma Si = 287.5°$, which are in good agreement with the MP4 and CCSD(T) results. The Si–C bond length at the MP2 level is slightly underestimated. In conclusion, B3LYP/6-31 + G(d) properly describes naturally as well as reverse-polarized silenes. Moreover, **21A** is a silene with a silicon–carbon single bond and with a structure intermediate between that of a regular Si=C bonded silene and the weak carbene–silylene complex of Lappert and co-workers.[11] It should largely be described by the resonance structures of type **II**, and we therefore call it a zwitterionic silene.

Cleavage of the Si=C bond in **21A** yields a carbene and a silylene which are both ground state singlets. At B3LYP/6-31 + G(d) and CCSD(T)/6-311 + G(2d,d,p) levels these cleavage products are 52.0 and 51.4 kcal mol^{-1} above **21A**, respectively. For **21B** and **21C** the corresponding B3LYP energies are 40.1 and 55.2 kcal mol^{-1}, in contrast to the complex

$[(CH)_2(NH)_2]C{-}Si[(NH)_2(CH)_2]$ for which the silicon–carbon bond dissociation energy was merely 3.2 kcal mol^{-1}.[11] We reason that alkyl and silyl substitution at Si in **21** gives single-bonded silenes that are stable to dissociation, even though the $Si{=}C$ bond dissociation energies in **21A**–**21C** are only 45–60% when compared to that of a normal $Si{-}C$ single bond ($\approx$90 kcal mol^{-1}).[34] The $Si{=}C$ bond dissociation energies are similar to those of tetraaminoethylenes (dissociation of $(H_2N)_2C{=}C(NH_2)_2$ requires 43.5 kcal mol^{-1} at the B3LYP/6-31 + G(d) level), which are moderately stable species when kept away from oxygen and moisture.[35] However, these dissociation energies may not fully represent the bond strengths of **21A**–**21C** because of the divalent state stabilization energies (DSSE) that preferentially stabilize the silylenes and carbenes relative to the radicals into which an ordinary $Si{-}C$ bonded compound dissociates.[34] For example, it is known that the double bond dissociation energies of $H_2Si{=}SiH_2$, $H_2Ge{=}SiH_2$, and $H_2Ge{=}GeH_2$ are smaller than the single bond dissociation energies of $H_3Si{-}SiH_3$, $H_3Ge{-}SiH_3$, and $H_3Ge{-}GeH_3$, as a result of DSSE.[36] The sum of the DSSEs of the silylene and carbene fragments of **21A**–**21C** are significant (59.1 (**21A**), 63.4 (**21B**), and 47.0 kcal mol^{-1} (**21C**) at the B3LYP/6-31 + G(d) level) and explain the low $Si{=}C$ bond dissociation energies.

However, the zwitterionic silenes can also be regarded as donor–acceptor complexes, and it was revealed by Frenking and co-workers that even strong dative bonds are not necessarily covalent.[37] For this reason, the electron density at the $Si{-}C$ bond critical point of **21A** was analyzed according to the Cremer–Kraka criteria.[30] This analysis shows that the $Si{-}C$ bond is covalent because the energy density $H(r_b)$ is negative at the bond critical point (-0.300 hartree Å^{-3} at the B3LYP/6-31 + G(d) level and -0.274 hartree Å^{-3} at the MP2/6-31 + G(d) level). In line with being a weakened $Si{-}C$ single bond, the $H(r_b)$ of **21A** is less negative than for $H_3Si{-}CH_3$ ($H(r_b) = -0.435$ hartree Å^{-3} at the B3LYP/6-31G + (d) level), and the electron density is reduced ($\rho(r_b) = 0.643$ e Å^{-3} in **21A** and 0.772 e Å^{-3} in $H_3Si{-}CH_3$). The rotational barrier of **21A** (4.2 kcal mol^{-1} at the B3LYP/6-31 + G(d) level) supports the conclusion of a silicon–carbon single bond. This is in contrast to the corresponding barrier of **1A**, which is calculated as 37 kcal mol^{-1} at the MCSCF/3-21G level.[38] For $Me_2Si{=}CH_2$ the rotational barrier has been estimated experimentally in the range 34–44 kcal mol^{-1}.[39, 40]

Silene geometries: The optimal geometries of a few representative silenes and 2-silenolates are shown in Figure 1, including both $Si^{\delta+}{=}C^{\delta-}$ and $Si^{\delta-}{=}C^{\delta+}$ polarized silenes. As seen when following one set, there is a connection between q(Si) and silicon–carbon bond length as well as ΣSi. Strong π electron donors at C cause silicon–carbon bond elongations and pyramidalizations of Si, whereas modest inductive electron withdrawal/donation exerted by the methyl/silyl substituents at Si leads to only small geometrical changes. Moreover, the carbon–nitrogen bonds in **16** and **21** are intermediate between $C{=}N$ double bonds and $C{-}N$ single bonds (the carbon–nitrogen bond distances in $H_2N{-}CH_3$ and $HN{=}CH_2$ at the B3LYP/6-31G + (d) level are 1.467 and 1.273 Å, respectively). Interestingly, the carbon–nitrogen bonds are generally shorter in **21** than in **16**. In contrast to methyl/silyl substituents at Si that do not lead to further geometric distortion of an already zwitterionic silene, strong π electron donor substituents at the Si of a zwitterionic silene further elongate and weaken the silicon–carbon bond.[11] This results from stabilization of the singlet state of the silylene leading to an even larger $\Sigma\Delta E_{ST}$ than in the silenes presently

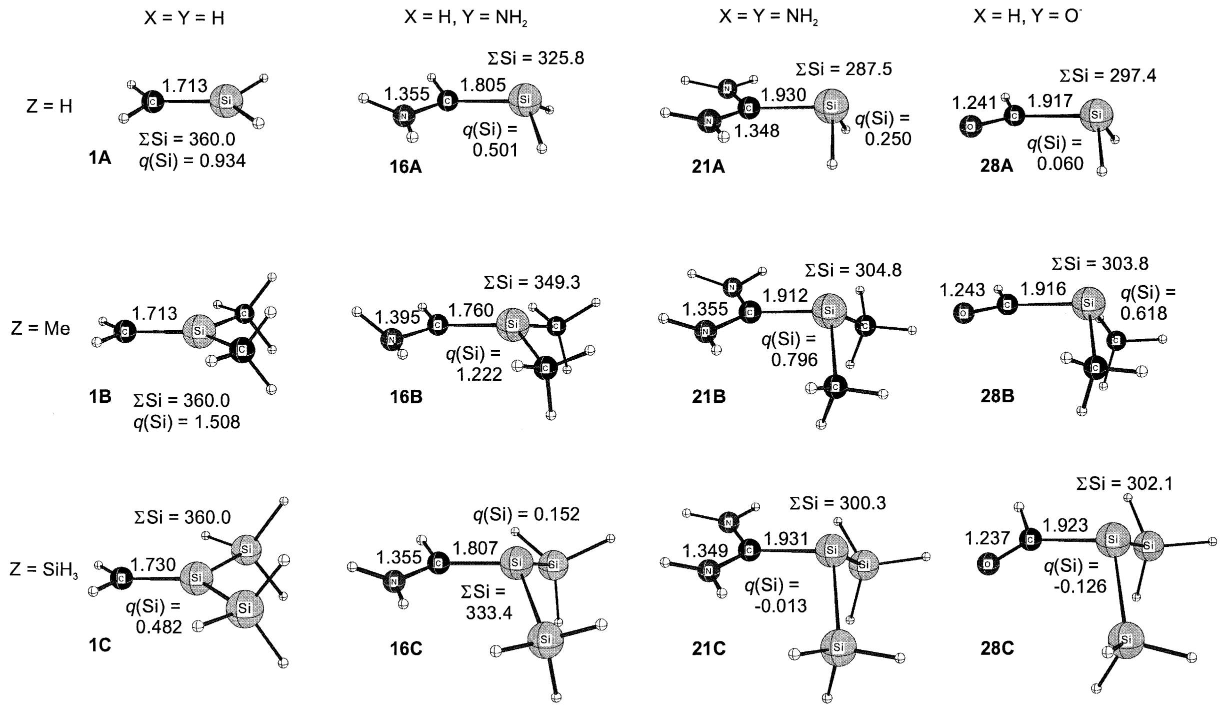

Figure 1. Optimal geometries and atomic charges at the Si atom of **1A**–**1C**, **16A**–**16C**, **21A**–**21C**, and **28A**–**28C** at the B3LYP/6–31 + G(d) level (distances [Å], angles [°], and charges [e]).

studied.[16] Ultimately, one reaches a point at which the silene should be described as a weak donor–acceptor complex between a carbene and a silylene (cf. Lappert's carbene–silylene complex).[11] However, π donor substituents on Si of a naturally polarized silene have no drastic structural effect.[11]

In addition to weakening the silicon–carbon bond, an amino, alkoxy, or halo substituent at the Si atom of a zwitterionic silene counteracts the reduction of the positive charge at this atom. Whereas q(Si) is 0.25 e in **21A**, it is 1.20 e in $F_2Si{=}C(NH_2)_2$. The connection between the electrophilicity and substitution at the Si atom was previously probed by Leigh and co-workers through laser flash photolytic studies of the reactivity of transient silenes towards MeOH.[4] For the silenes investigated it was found that inductively withdrawing substituents on Si increase the reactivity. In **21C**, on the other hand, the silene Si atom is essentially neutral (−0.01 e), so that it will be less electrophilic and this silene should have a fundamentally different reactivity than $Si^{\delta+}{=}C^{\delta-}$ polarized silenes. Indeed, unexpected reactivities for Si=C bonded compounds were recently detected by the groups of Sekiguchi and Kira when investigating H_2O and MeOH addition to persilyl-substituted 1-silaallene and to a 4-silatriafulvene.[5e, 41] It was found that the O atom adds to the C and not to the Si end of the Si=C bond, supporting a partial reversal of the Si=C bond polarity. In support of this changed reactivity, Apeloig and co-workers very recently found that silenes with substituents that strongly reduce the silene polarity have high energy barriers for addition of H_2O.[42]

With regard to the 2-silenolates **28A**–**28C**, the optimal geometries of these species are also best represented by a resonance structure of type **II** (Figure 1). The variation in geometry with Z is only small so that this conclusion applies to all 2-silenolates. The carbon–oxygen bond distances at the B3LYP/6-31+G(d) level are slightly longer than in $H_2C{=}O$ (1.209 Å), but considerably shorter than in $H_3C{-}OH$ (1.425 Å). The calculated structures are similar to the X-ray crystal structure recently determined by us.[9]

The Si atomic charges of the 2-silenolates (0.06 e (**28A**), 0.62 e (**28B**), and −0.13 e (**28C**)) also resemble those of the silyl anions H_2MeSi^- (0.02 e), Me_3Si^- (0.59 e), and $(H_3Si)_2MeSi^-$ (−0.11 e). Although the agreement is excellent in q(Si) of the silyl anions and 2-silenolates, this comparison is not fully justified, since it assumes that the extent of inductive electron withdrawal from Si by a CHO group and by a methyl group are similar.[43, 44] Nevertheless, the geometry data and the charge distribution of the 2-silenolates indicate that these species are fully described by a resonance structure with the negative charge localized at Si. This is somewhat surprising from electronegativity reasons, but the C=O π bond is much stronger than the Si=C π bond. Thus, 2-silenolates and zwitterionic silenes are closely related, since they both are dominated by type **II** resonance structures. Consequently, these species should have similar reactivities.

A polar solvent environment has, according to PCM-B3LYP/6-31+G(d) calculations, only a modest influence on geometries of 2-silenolates, zwitterionic, and naturally polarized silenes. In a highly polar medium with the same dielectric constant as water, **21A** and **28A** have $r_{Si=C}$ and ΣSi values of 1.951 and 1.889 Å, and 272.5 and 285.0°, respectively, which are similar to the corresponding gas-phase values (Figure 1). In the naturally polarized silene **1A**, the silicon–carbon distance is 1.730 Å in water, as compared to 1.713 Å in the gas phase.

Reversed silicon–carbon bond polarization seems to have no distinct and predictable effect on the relative stabilities of various silene conformers. However, the relative stability of a particular conformation is also influenced by, for example, steric demand and does not solely reflect the energetic influence of reversed polarization.

Dependence of $r_{Si=C}$ and ΣSi on q(Si) and ΔE_{ST}: One aim of the study was to probe the connection between geometric structure and reversed silicon–carbon bond polarization. As an approximation it is assumed that q(Si) within each of the three separate sets of silenes can be used as a measure of the extent of reversed polarization. This neglects differences in the inductive electron withdrawal from Si by the various CXY units, and also the change in electronegativity of Si when going from an sp^2-hybridized Si in a planar silene to an sp^3-hybridized Si in a pyramidalized one. Bergman and Hinze determined the sp^2 and sp^3 hybrid orbital electronegativities of Si according to the Pauling scale as 2.44 and 2.23, respectively.[43] This small difference may justify neglect of the difference in inductive electron withdrawal from Si exerted by, for example, a methyl group in a silene with a planar versus pyramidal Si atom.

For each set of silenes, the dependence of $r_{Si=C}$ on q(Si) is described by a separate curve (Figure 2A). Each of these curves can be partitioned in two parts, with good linear correlations between q(Si) and $r_{Si=C}$ for the parts of the curves that correspond to pyramidalized structures. For the planar silene structures, there is no correlation between Si=C bond length and q(Si). It is noteworthy that the neutral and anionic species contained in the study are described by the same curves, indicating that silenes and, for example, 2-silenolates are closely related.

The Si atoms also become progressively more pyramidal with lower q(Si), and they level at values of ΣSi within 280–300° (Figure 2B). The dependence of ΣSi on q(Si) is sigmoidal as expected, since 360° is the upper limit and the values of ΣSi for silyl anions should be the lower limit. Indeed, at the B3LYP/6-31+G(d) level, the H_2MeSi^-, $(H_3Si)_2MeSi^-$, and Me_3Si^- ions have ΣSi values of 289.2°, 292.2°, and 293.7° that are similar to the values of strongly zwitterionic (reverse-polarized) silenes. This supports the interpretation that the zwitterionic resonance structure **II** is dominant in the description of the electronic structure of silenes such as **21**. The point along the q(Si) coordinate at which the pyramidalization starts is also the breakpoint on the $r_{Si=C}$ versus q(Si) plot.

The differences in the extent of pyramidalization of silenes with the same X and Y but with different Z groups are small, as was similarly noted above for the three silyl anions H_2MeSi^-, Me_3Si^-, and $(H_3Si)_2MeSi^-$. Consequently, the lower parts of the curves level at similar values, and the small variation in the ΣSi could be caused by steric rather than electronic reasons because both set **B** and **C** level at values of ΣSi that are higher than that of set **A**. This also agrees with our finding that ΣSi in the crystal structure of the potassium 1-*t*Bu-2,2-bis(trimethylsilyl)-2-silenolate (317.8°) is larger than in the

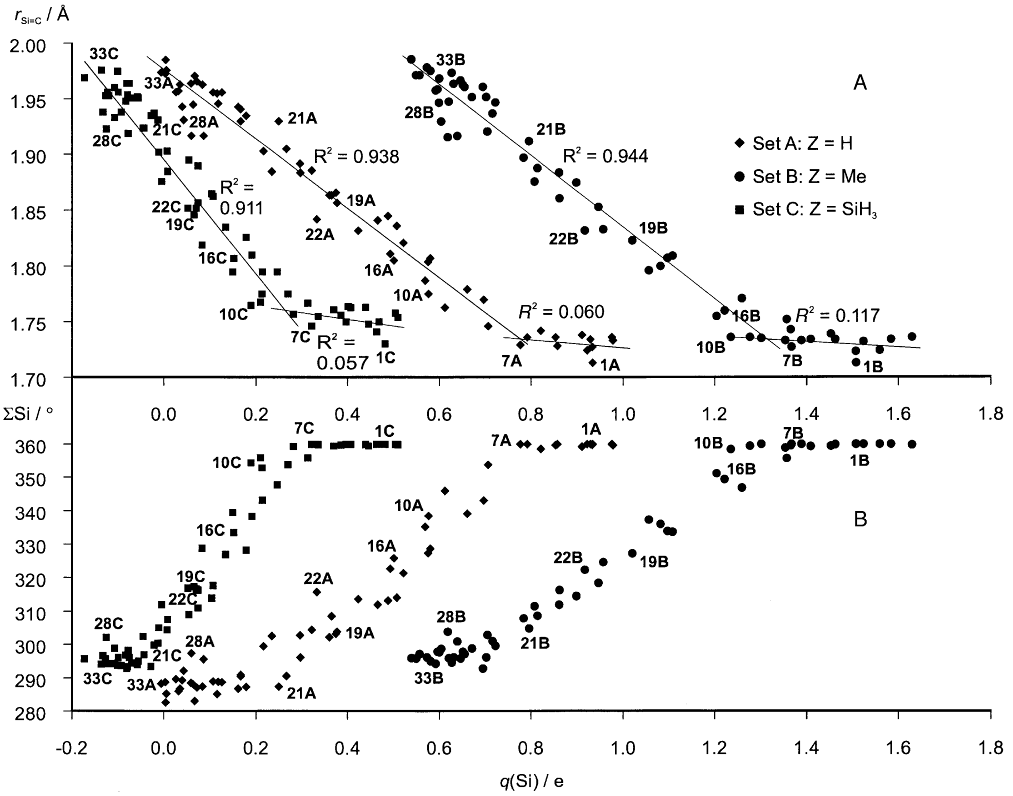

Figure 2. Dependence of A) Si=C bond length ($r_{Si=C}$) and B) the sum of valence angles at Si (ΣSi) on the atomic charge at Si (q(Si)) based on B3LYP/6-31+G(d) calculations (atomic charges from natural population analyses).

calculated structure of a $K^+(OMe_2)_3$-coordinated 2-silenolate in which the TMS groups are changed to SiH_3 groups (307.0°).[9] However, Liang and Allen also showed that the substituent electronegativity determines the extent of *trans* bending/pyramidalization of Group XIV A=A double bonds, with electronegative substituents leading to more *trans*-bent/pyramidal structures than less electronegative substituents.[22] In line with this finding, $F_2Si=C(NH_2)_2$ has a ΣSi value of 278.5° at the B3LYP/6-31+G(d) level (i.e., slightly lower than those of **21 A**–**21 C**).

A connection between reversed polarization and CGMT theory should exist because of the breakpoint in the curves relating $r_{Si=C}$ and ΣSi to q(Si), and because the CGMT theory shows that pyramidalizations in heavy alkenes set in when $\Sigma\Delta E_{ST} \geq f(E_{\sigma+\pi})$ with $f = ½[1 + (q_1 + q_2)/2] + \alpha q_1 q_2$ (for the meaning of α, q_1, and q_2 see the introduction).[16, 17] To probe the connection between reversed Si=C bond polarization and the CGMT theory, q(Si) was plotted against $\Sigma\Delta E_{ST}$ (Figure 3), in which $\Sigma\Delta E_{ST}$ is the sum of the singlet–triplet energy gaps of the interacting silylene and carbene units of the silene. Both the $\Sigma\Delta E_{ST}$ calculated at the carbene and silylene geometries frozen as in the corresponding silenes ($\Sigma\Delta E_{ST}$(sp)), and at the optimal geometries of the silylenes and carbenes in their singlet and triplet states ($\Sigma\Delta E_{ST}$(opt)) are given. For a listing of the $\Sigma\Delta E_{ST}$ values of the carbene and silylene fragments of **1 A**–**21 A** see the Supporting Information. As can be seen, q(Si) depends linearly on $\Sigma\Delta E_{ST}$, and the correlation is particularly good with $\Sigma\Delta E_{ST}$(sp) (Figure 3 A). A fair correlation is obtained with $\Sigma\Delta E_{ST}$(opt) (Figure 3 B). A possible explanation for the better correlation with $\Sigma\Delta E_{ST}$(sp) than $\Sigma\Delta E_{ST}$(opt) could be found from an analysis of the interacting orbitals of the carbene and silylene fragments.

A silene can be pictured as a combination of one triplet silylene with both unpaired electrons having α spins and one triplet carbene with both unpaired electrons having β spins (Figure 4). Since it is mainly the energy of the second SOMO of the triplet carbene (i.e., the pπ-type orbital) that is raised when going from a carbene with a low ΔE_{ST} to one with a large ΔE_{ST} (Figure 4 B), the filled π(SiC) orbital of the silene will become progressively less localized at C and more localized at Si. The increased contribution of the 3pπ(Si) AO in this filled MO will lead to a larger electron density at Si and this atom gradually becomes more similar to the Si of silyl anions. Since the electronic structure, as reflected by orbital energies and ΔE_{ST}, at the geometries that the carbene and silylene fragments adopt in the silenes determines the relative charge transfer to Si, a better correlation between q(Si) and $\Sigma\Delta E_{ST}$ is obtained with $\Sigma\Delta E_{ST}$(sp) than with $\Sigma\Delta E_{ST}$(opt) (Figure 3 A versus Figure 3 B). Because of the linear correlation between q(Si) and $\Sigma\Delta E_{ST}$, the geometric parameters depend on $\Sigma\Delta E_{ST}$ in the same way as they depend on q(Si) (Figure 5). As the correlation between q(Si) and $\Sigma\Delta E_{ST}$ is better for $\Sigma\Delta E_{ST}$(sp) than for $\Sigma\Delta E_{ST}$(opt), this also applies for the correlation between the geometrical parameters $r_{Si=C}$ and ΣSi and $\Sigma\Delta E_{ST}$ (Figure 5 A and B versus Figure 5 C and D). For silenes with pyramidal Si, there is a linear dependence of $r_{Si=C}$ and ΣSi on $\Sigma\Delta E_{ST}$(sp), whereas the correlation is truly modest with $\Sigma\Delta E_{ST}$(opt).

According to CGMT theory, the breakpoint corresponds to the point at which $\Sigma\Delta E_{ST} \approx f(E_{\sigma+\pi})$,[17] and for pyramidalized

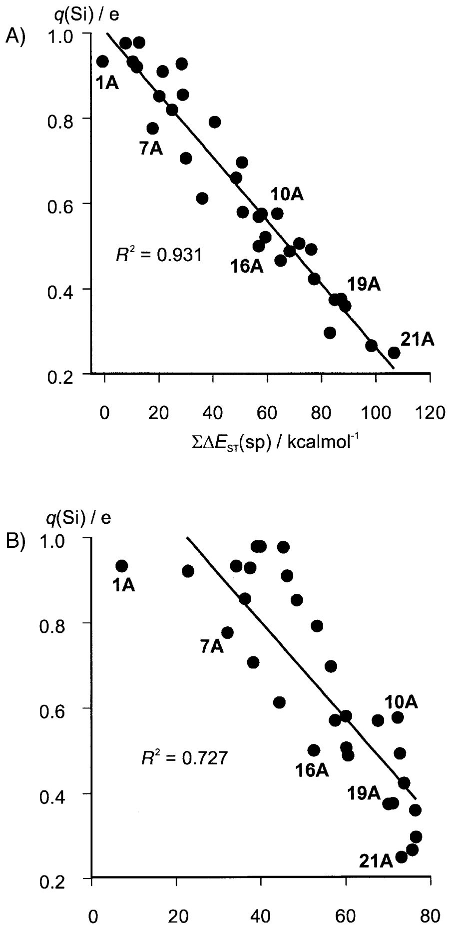

Figure 3. Atomic charges at Si (q(Si)) as a function of the sum of the singlet–triplet energy splittings of the carbene and silylene fragments ($\Sigma\Delta E_{ST}$) of neutral silenes **1A**–**21A**. A) $\Sigma\Delta E_{ST}$ calculated at geometries of the silylene and carbenes frozen as in the corresponding silenes ($\Sigma\Delta E_{ST}$(sp)), and B) $\Sigma\Delta E_{ST}$ calculated at the optimal geometries of the silylene and carbenes of the corresponding silenes ($\Sigma\Delta E_{ST}$(opt)). Results obtained from (U)B3LYP/6–31 + G(d) calculations.

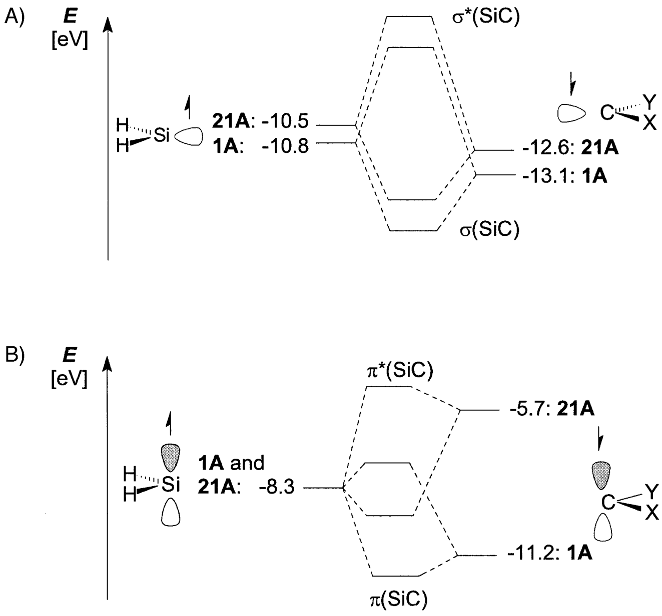

Figure 4. Orbital interaction for the formation of A) σ(SiC), σ*(SiC) MOs and B) π(SiC) and π*(SiC) MOs from one triplet H_2Si: silylene and one triplet XYC: carbene. Orbital energies from UHF/6–31 + G(d)//B3LYP/6–31 + G(d) calculations on carbene and silylene structures taken as in **1A** and **21A**. Spin contaminations of the UHF wave functions were small (maximum $<S^2> \leq 2.004$).

silenes $\Sigma\Delta E_{ST} > f(E_{\sigma+\pi})$.[45] The derivation of Equation (1) assumed freely geometry-optimized carbenes and silylenes in their singlet and triplet states. A result in agreement with Equation (1) is also only observed with $\Sigma\Delta E_{ST}$(opt), and the validity is only approximate. For planar silenes near the breakpoint, and for slightly pyramidalized silenes, $\Sigma\Delta E_{ST}$(opt) is just somewhat smaller than $f(E_{\sigma+\pi})$, whereas for planar silenes $\Sigma\Delta E_{ST}(\text{opt}) < f(E_{\sigma+\pi})$, and for strongly pyramidal silenes $\Sigma\Delta E_{ST}(\text{opt}) > f(E_{\sigma+\pi})$. For example, for the planar silene **7A**, $\Sigma\Delta E_{ST}$(opt) is 32.5 kcal mol^{-1} and $f(E_{\sigma+\pi})$ is 60.3 kcal mol^{-1} at the B3LYP/6-31 + G(d) level. On the other hand, for **10A** with $\Sigma Si = 338.5°$, $\Sigma\Delta E_{ST}$(opt) is 72.6 kcal mol^{-1}, and $f(E_{\sigma+\pi})$ is 64.1 kcal mol^{-1}, and for the strongly pyramidal **21A** ($\Sigma Si = 287.5°$) $\Sigma\Delta E_{ST}$(opt) is 73.4 kcal mol^{-1} and $f(E_{\sigma+\pi})$ is 70.1 kcal mol^{-1}. For **8A**, which is planar but close to the breakpoint, $\Sigma\Delta E_{ST}$(opt) is 53.5 kcal mol^{-1} and $f(E_{\sigma+\pi})$ is 65.9 kcal mol^{-1}. However, even for the slightly pyramidal **11Aa** with $\Sigma Si = 355.5°$, the $\Sigma\Delta E_{ST}$(opt) is 44.7 kcal mol^{-1} and $f(E_{\sigma+\pi})$ is 63.1 kcal mol^{-1}. Thus, the application of Equation (1) to assess exactly when pyramidalization of silenes sets in seems difficult. Similar results are obtained at the MP2/6-31G + (d) level.

According to Carter and Goddard, the $\Sigma\Delta E_{ST}$ can also be used to deduce the bond dissociation energy E_{diss} of a substituted alkene XYC=CX'Y' [Eq. (2)], where E_{int}(C=C) is the intrinsic C=C bond energy, obtained from ethylene as 172 ± 2 kcal mol^{-1}.[16] This suggests a linear relationship between the $\Sigma\Delta E_{ST}$ values of the two carbene fragments and the C=C bond dissociation energy of the substituted alkene, and this relationship has indeed been verified computationally for substituted alkenes and disilenes.[19, 46] As seen in Figure 6 this relationship also applies to the neutral silenes **1A**–**21A** for which $\Sigma\Delta E_{ST}$ values have been calculated.

$$E_{diss}(XYC{=}CX'Y') = E_{int}(C{=}C) - [\Delta E_{ST}(CXY) + \Delta E_{ST}(CX'Y')] \qquad (2)$$

Thermodynamic stability in relation to reversed polarization: Silenes normally dimerize in the absence of reaction partners,[1] and the aptitude for dimerization as a function of extent of reversed Si=C bond polarization should be of interest. Gusel'nikov et al. recently found that substituents R influence the dimerization energy (E_{dim}) of $R_2Si{=}CH_2$ silenes into 1,3-disilacyclobutanes.[47] Silyl groups lower E_{dim} by ≈4 kcal mol^{-1} when compared to the parent silene ($E_{dim} = -78.3$ kcal mol^{-1} at the MP4/6-311G(d)//MP2/6-31G(d) level). On the other hand, when R = F, E_{dim} is even more exothermic by ≈37 kcal mol^{-1}.

Substitution at the C end of the silene also affects the dimerization energies. We considered both the head-to-tail dimerization into 1,3-disilacyclobutanes and the head-to-head dimerization into 1,2-disilacyclobutanes (Figure 7). Only neutral $H_2Si{=}CXY$ silenes were included in this part of the

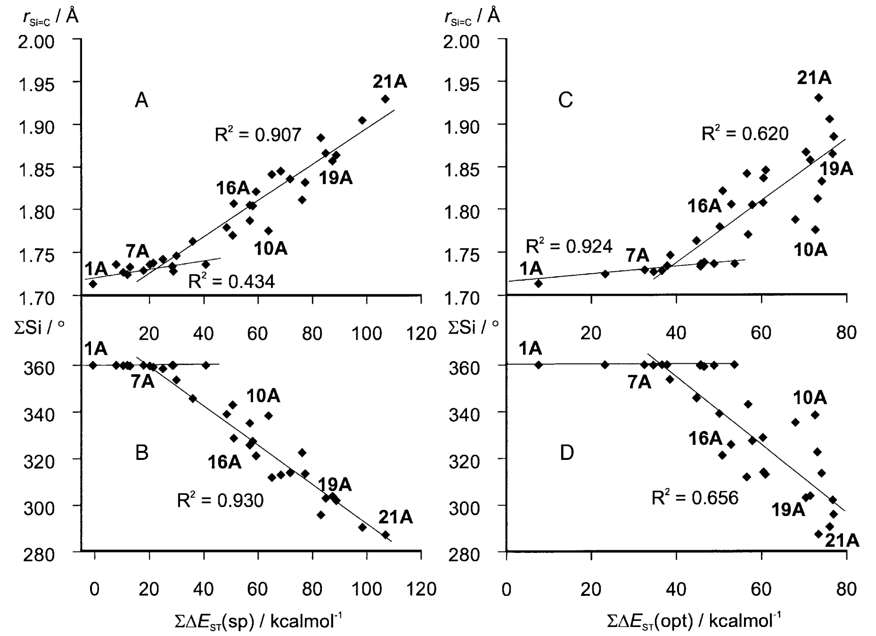

Figure 5. Dependence of (A and C) Si=C bond length ($r_{Si=C}$), and (B and D) the sum of valence angles at Si (ΣSi) of **1A**–**21A**, on the sum of the singlet–triplet energy splittings of the carbene and silylene fragments ($\Sigma\Delta E_{ST}$) at the B3LYP/6-31 + G(d) level. A) and B) $\Sigma\Delta E_{ST}$ calculated at geometries of the silylene and carbenes frozen as in the corresponding silenes ($\Sigma\Delta E_{ST}$(sp)). C) and D) $\Sigma\Delta E_{ST}$ calculated at the optimal geometries of the silylene and carbenes of the corresponding silenes ($\Sigma\Delta E_{ST}$(opt)).

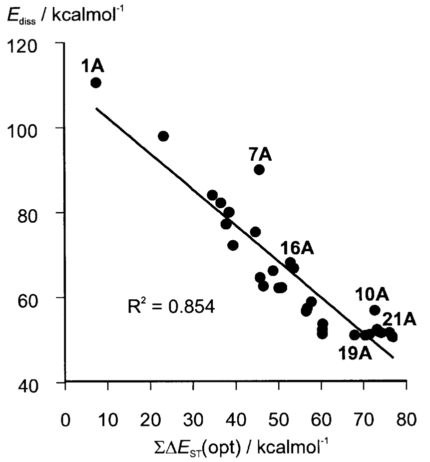

Figure 6. Dependence of Si=C bond dissociation energies of silenes **1A**–**21A** on the sum of the singlet–triplet energy splittings ($\Sigma\Delta E_{ST}$(opt)) of the interacting carbene and silylene fragments. Results from B3LYP/6-31 + G(d) calculations.

study. A screening of the relative energies was done at the B3LYP/3-21G(d) level in cases for which several diastereomers of a particular 1,2- or 1,3-disilacyclobutane exist, or in cases for which the dimer has conformational flexibility. The most stable conformer was further optimized with B3LYP/6-31 + G(d). Certain conformers of some dimers (e.g., that of **21A**) have intramolecular hydrogen bonds, and inclusion of these in the analysis would bias the dependence of E_{dim} on q(Si). Such conformers were therefore excluded, and those of lowest energy that are not hydrogen-bonded were included instead. Previously, Apeloig and Karni found that the variation in thermodynamic stability toward dimerization was small among different silenes,[2] but they used only monosubstituted silenes, and the strongest π electron donors were hydroxy and siloxy groups. The present set of silenes provides a more extensive test whether reversed silicon–carbon bond polarization enhances the thermodynamic stability toward dimerization.

At the B3LYP/6-31 + G(d) level the energies released upon head-to-tail dimerization of $H_2Si{=}C(NH_2)_2$ (**21A**) and $H_2Si{=}C(NH_2)(OH)$ (**20A**) are 27.3 and 31.2 kcal mol⁻¹, respectively, and these energies are closer to that of ethylene (E_{dim} = – 16.7 kcal mol⁻¹) than to that of **1A** (E_{dim} = – 79.3 kcal mol⁻¹). The 4-silatriafulvene of Kira and co-workers[5] releases 46.4 and 45.2 kcal mol⁻¹ upon head-to-tail and head-to-head dimerization, indicating that this silene is less influenced by reversed polarization than **21A**. It is noteworthy that there is no apparent preference for head-to-tail or head-to-head dimerization, neither for naturally polarized nor reverse-polarized (zwitterionic) silenes (Figure 7). The dependence of E_{dim} on q(Si) is not linear, and the reduction in E_{dim}, when compared to that of **1A**, is small for silenes that are moderately affected by reversed polarization (e.g., $H_2Si{=}CHOH$ for which E_{dim} is – 63.6 and – 62.7 kcal mol⁻¹ for head-to-tail and head-to-head dimerization, respectively).

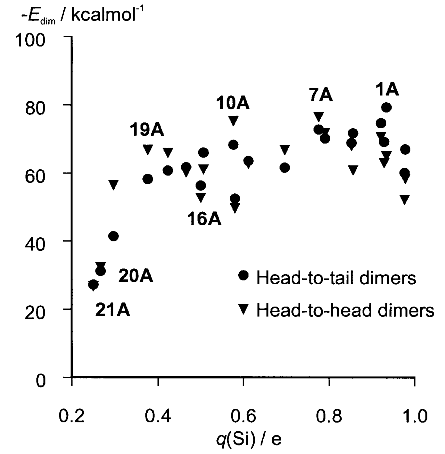

Figure 7. Energies for dimerization of **1A**–**21A** into the corresponding head-to-tail and head-to-head dimers. Results from B3LYP/6-31 + G(d) calculations.

Silyl substituents on Si lowers q(Si) as compared to H, and **21C** should be the neutral silene in this study with the least electrophilic Si and lowest tendency to form dipole–dipole complexes. In addition, E_{dim} of **21C** at the B3LYP/6-31G + (d) level is even lower than that of **21A** (– 13.7 kcal mol⁻¹ for the head-to-tail dimer). The methyl group has the opposite effect, as **21B** releases 40.0 kcal mol^{-1} upon dimerization. Strongly electron-withdrawing substituents at Si lead to even higher dimerization energies (vide infra). Since such substituents also increase the electrophilicity and counteract the reduction of the silicon–carbon bond dipole moment caused by reversed polarization, they presumably lower the kinetic stability of such silenes towards both dimerization and nucleophilic attack. It is noteworthy that the same trend in E_{dim} is followed by the zwitterionic silenes **21** as the naturally polarized silenes previously studied by Gusel'nikov and co-workers.[47]

Dimerization is only one of the reaction channels leading away from the silene; the others are various rearrangements. A detailed exploration of all possible rearrangement pathways is outside the scope of the present study. Instead we use relative energies of $H_2Si{=}CX_2$ as compared to $X_2Si{=}CH_2$ silenes (X = F, Cl, SH, OH, or NH_2) as rough indicators of their stabilities, and presumably also their aptitudes to rearrange. The effect of substituents on the Si=C bond energy was previously determined by Apeloig and Karni through isodesmic reactions.[2]

Photochemically as well as thermally initiated exchange of the positions of TMSO(C) and TMS(Si) substituents has been observed by Brook and co-workers.[48] Clearly, the stronger Si–O and Si–F bonds (relative to C–O and C–F bonds) extensively stabilize $(HO)_2Si{=}CH_2$ and $F_2Si{=}CH_2$ over $H_2Si{=}C(OH)_2$ and $H_2Si{=}CF_2$ (Table 2), similarly as was concluded by Apeloig and Karni.[2] However, the energy difference between $(H_2N)_2Si{=}CH_2$ and $H_2Si{=}C(NH_2)_2$ is smaller and it approaches the energy difference between $Me_2Si{=}CH_2$ and $H_2Si{=}CMe_2$. Alkyl substituents on the C atom have no rearrangement aptitude, and one could hope that the same applies to amino groups at this position.

The dimerization energies are considerably higher for 1,1-dihalo- or 1,1-dihydroxy-substituted silenes than for the isomeric 2,2-disubstituted variants (Table 2). The pattern of increased thermodynamic stability towards dimerization upon increased importance of reversed polarization is thus elusive for some silenes. Because of the particularly large differences in relative energies, 2,2-dialkoxy, disiloxy, or dihalo-substituted silenes may rearrange to their 1,1-disubstituted isomers, and subsequently dimerize. This process should be less likely for 2,2-diamino-substituted silenes.

Silene inversion: Since the charge of Si in zwitterionic silenes resembles that of Si in silyl anions, the structure around this atom in these silenes and in silyl anions should be influenced by substituents similarly. Interesting properties of both types of species are their pyramidal structures and inversion barriers (E_{inv}). It is known that electron-withdrawing substituents increase E_{inv} of silyl anions,[49] in accordance with a Walsh analysis of AX_3 species with eight valence electrons.[50] The inversion barriers of silenes with pyramidal Si atoms are influenced in the same way, as revealed by B3LYP, MP2, and CCSD(T) calculations of $Z_2Si{=}C(NH_2)_2$ silenes **21A**–**21I** (Table 3).

Table 2. B3LYP/6–31 + G(d)-computed data of $H_2Si{=}CX_2$ and $X_2Si{=}CH_2$ silenes.[a]

	$H_2Si{=}CX_2$					$X_2Si{=}CH_2$					
X	Sym	$r_{Si=C}$	ΣSi	E_{dim}	q(Si)	Sym	$r_{Si=C}$	ω(Si=C)[b]	q(Si)	E_{dim}	E_{rel}[c]
H	C_{2v}	1.713	360.0	– 79.3	0.934	–	–	–	–	–	–
SiH_3	C_{2v}	1.715	360.0	– 68.3	1.111	C_{2v}	1.730	0.0	0.482	– 68.9	1.0
Me	C_{2v}	1.728	360.0	– 63.4	0.869	C_{2v}	1.713	0.0	1.508	– 78.4	– 16.6
NH_2	C_s	1.930	287.5	– 27.3	0.250	C_2	1.704	15.8	1.862	– 80.5	– 34.0
SH	C_1	1.736	360.0	– 60.1	0.976	C_2	1.707	7.1	1.135	– 88.8	– 43.8
Cl	C_{2v}	1.734	360.0	– 69.2	0.929	C_{2v}	1.696	0.0	1.325	– 98.0	– 69.1
OH	C_s	1.884	296.1	– 41.4	0.297	C_2	1.698	0.0	2.024	– 97.6	– 58.2
F	C_s	1.775	338.5	– 68.4	0.576	C_{2v}	1.685	0.0	2.089	– 109.9	– 86.6

[a] Data includes bond lengths [Å], angles [°], and energies [kcal mol^{-1}]. [b] ω(Si=C) corresponds to the dihedral angle X-Si-C-H. [c] Energy difference $E[X_2Si{=}CH_2] - E[H_2Si{=}CX_2]$.

Table 3. Geometry, charge, and energy data for $Z_2Si{=}C(NH_2)_2$ silenes.[a]

Silene	Sym	E_{inv} B3LYP/ 6–31 + G(d)	E_{inv} CCSD(T)/ 6–311 + G(d,p)// B3LYP/ 6–31 + G(d)	E_{inv} MP2/ 6–311 + G(d,p)// B3LYP/ 6–31 + G(d)	$r_{Si=C}$	ΣSi	q(Si)	E_{diss}[b]	DSSE[c]	$\Sigma\Delta E_{ST}$(opt)	ω(X–Si–C–N)[d]
21A, $H_2Si{=}C(NH_2)_2$	C_s	10.3	6.6	4.3	1.930	287.5	0.25	52.0	59.1	73.4	14.7
21B, $Me_2Si{=}C(NH_2)_2$	C_s	6.0	3.0	0.4	1.912	304.8	0.80	40.1	63.4	81.4	14.3
21C, $(H_3Si)_2Si{=}C(NH_2)_2$	C_s	6.4	5.1	3.5	1.931	300.3	– 0.01	55.2	47.0	61.1	13.7
21D, $F_2Si{=}C(NH_2)_2$	C_1	38.4	34.9	31.8	2.080	278.5	1.20	30.5	94.8	127.1	13.2
21E, $Cl_2Si{=}C(NH_2)_2$	C_s	33.8	29.0	26.3	2.030	287.5	0.74	39.4	79.9	105.9	13.4
21F, $(F_3C)_2Si{=}C(NH_2)_2$	C_s	25.1	–	23.5	1.974	286.6	0.68	62.7	64.6	80.7	13.7
21G, $(HO)_2Si{=}C(NH_2)_2$	C_1	29.7	28.2	25.9	1.992	284.0	1.06	35.2	91.4	116.9	6.8
21H, $(H_2N)_2Si{=}C(NH_2)_2$	C_s	19.3	17.0	14.8	1.965	295.7	0.99	20.1	89.0	109.9	8.6
21I, $Ph_2Si{=}C(NH_2)_2$	C_1	7.8	–	6.3	1.938	303.5	0.83	40.4	62.2	79.4	17.9

[a] Data includes distances [Å], angles [°], charges [e], and energies [kcal mol^{-1}]. [b] Energy required for dissociation into Z_2Si: and $(H_2N)_2C$: fragments. [c] Sum of the divalent state stabilization energies of the X_2Si and $C(NH_2)_2$ unit of each silene, calculated in accordance with ref. [34]. [d] Dihedral angle measuring the twist of the Z_2Si and $C(NH_2)_2$ planes relative to each other at the transition state for inversion.

A rise in E_{inv} on going from H to F substituents on Si of 4-silatriafulvene was reported by Kira and co-workers.[5c] The 4,4-difluoro-4-silatriafulvene has an E_{inv} of 10.4 kcal mol^{-1} at the MP2/6-311++G(d,p) level, whereas this barrier is merely 1.4 kcal mol^{-1} for the parent 4-silatriafulvene. One could argue that silenes with even higher inversion barriers (e.g., **21F**) have difficult electronic structures, but T_1-diagnostics of the CCSD/6-311+G(d)//B3LYP/6-31+G(d) wave function reveal that both ground and transition states are properly described by a single-reference method.[51] It is noteworthy that the more precise CCSD(T) values are flanked by the B3LYP and MP2 values; the last two methods presumably give slightly too high and low E_{inv} values, respectively. The inversion barrier in **28A** is 13.1 kcal mol^{-1} at the B3LYP/6-31+G(d) level (i.e., slightly higher than that of **21A**), and the E_{inv} of 2-silenolates should be tunable by substitution in the same way as those of neutral zwitterionic silenes.

From Table 3 it becomes apparent that there is a linear correlation between ΣSi and E_{inv} ($R^2 = 0.737$), whereas there is a poor correlation between q(Si) and E_{inv} ($R^2 = 0.381$). For example, **21B** has a more positively charged Si atom than in **21F**, but E_{inv} of the latter compound is fourfold higher. Trifluoromethyl substituents therefore seem appropriate if one searches for a silene with a high E_{inv}, without an excessively positive Si atom. The same applies to Cl substituents. An interesting feature of the transition states for inversion of **21A**–**21I** is the slight twisting ω(X-Si-C-N) of the planes of the silylene and carbene units (Table 3).

A rewarding property of CF_3 substituents is that they increase the energy for dissociation into carbenes and silylenes, in contrast to other substituents that raise E_{inv}. One could initially assume a connection between the silicon–carbon bond lengths of **21A**–**21I** and their dissociation energies (E_{diss}), but there is none (an attempted linear correlation gives $R^2 = 0.14$). However, the $\Sigma\Delta E_{\mathrm{ST}}$ can be used to estimate E_{diss} as proposed by Carter and Goddard,[16] even though the linear correlation between these two properties is worse for **21A**–**21I** ($R^2 = 0.601$) than for **1A**–**21A** ($R^2 = 0.854$, Figure 6). When the two sets of silenes are added together the correlation factor becomes $R^2 = 0.823$. Furthermore, a perfect linear correlation between DSSE and $\Sigma\Delta E_{\mathrm{ST}}$ of the carbene fragments CXY of substituted alkenes has previously been found,[46] and a good linear correlation between these properties also exists for silenes **21A**–**21I** ($R^2 = 0.984$). As seen in Table 3, neither the $\Sigma\Delta E_{\mathrm{ST}}$ nor DSSE of $(F_3C)_2Si{=}C(NH_2)_2$ (**21F**) are excessively high, and therefore, this silene should have a considerable E_{diss}. Those of the silenes **21A**–**21I** with high $\Sigma\Delta E_{\mathrm{ST}}$(opt) and DSSE generally have low E_{diss}.

The inversion barriers of **21D**–**21G** (Table 3) should be sufficiently high to prevent inversion at ambient temperatures. Since a few chiral silyl anions have been reported,[52] one can postulate that silenes and 2-silenolates with Si as a chiral center are also possible. A few examples of such species are given in Figure 8 together with their E_{inv}, $r_{\mathrm{Si=C}}$, ΣSi, and q(Si) values. The silicon–carbon bonds in these compounds are single bonds, so their rotational barriers are low and they should resemble that of **21A** which is 4.2 kcal mol^{-1} at the B3LYP/6-31+G(d) level. As was similarly found with **21A** and **28A**, the inversion barrier is higher in the 2-silenolate than in the 2,2-diamino-silene with the same Si substituents.

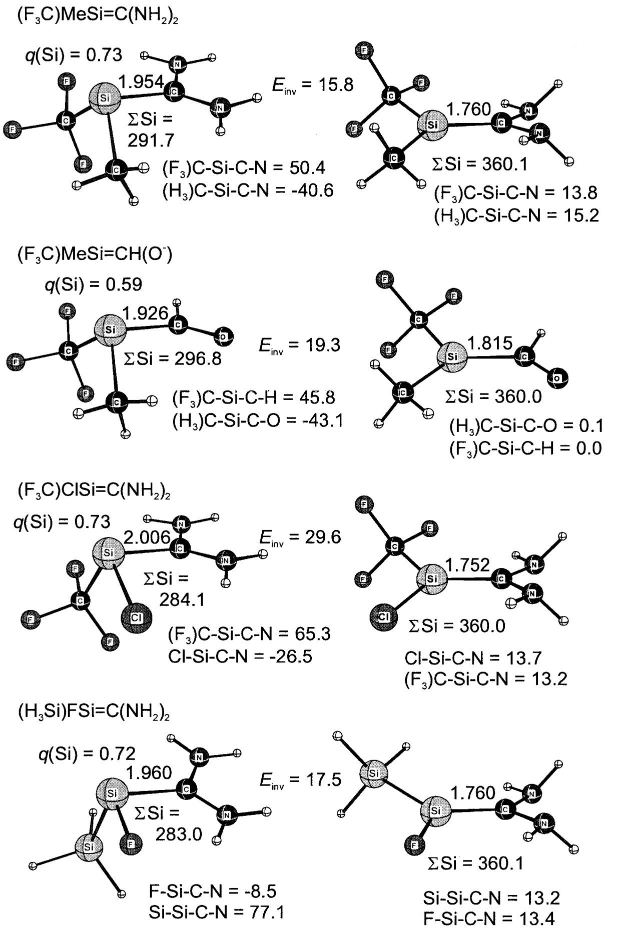

Figure 8. Optimal geometries of three $XYSi{=}C(NH_2)_2$ silenes and one $XYSi{=}CH(O^-)$ silenolate, geometries of their transition states for inversion, energies for inversion (E_{inv}), and atomic charges at Si (q(Si)). Results from B3LYP/6-31+G(d) calculations (bond lengths [Å], angles [°], energies [kcal mol^{-1}], and charges [e]).

If the two C substituents differ from each other, as in a chiral 2-silenolate, then it is likely that both E and Z isomers of the chiral species are populated at temperatures used in organic synthesis, unless one of them is destabilized by, for example, steric congestion. The rotational flexibility is a drawback but stems from the fact that a chiral silene/2-silenolate is only achievable at the expense of the Si=C double bond. From the results presented in Table 3, we can conclude that most suitable Si substituents seem to be two fluorinated alkyl groups of different size. However, the generation of a chiral zwitterionic silene or 2-silenolate based on this framework is likely to be synthetically challenging.

Conclusion

A computational investigation was carried out on silenes $Z_2Si{=}CXY$ (Z = H, Me, or H_3Si; X = H, SH, Cl, F, OH, or NH_2; Y = H, SH, Cl, F, OH, NH_2, O^-, S^-, or NH^-). These were grouped into three sets depending on Z: set **A** with Z = H, set **B** with Z = Me, and set **C** with Z = SiH_3. It was found that the inexpensive hybrid DFT method B3LYP is equally able to describe the geometries of both $\mathrm{Si}^{\delta+}{=}\mathrm{C}^{\delta-}$ and $\mathrm{Si}^{\delta-}{=}\mathrm{C}^{\delta+}$ polarized silenes as CCSD(T). The calculations reveal that the Si=C bond gradually elongates and the Si atom pyramidalizes as reversed polarization becomes increasingly more important. Silenes with two strongly π electron-donating substituents at C are fully described by zwitterionic resonance structures of type **II** (Scheme 1). Such silenes have Si–C single bonds and distinctly pyramidal Si atoms with ΣSi similar to silyl anions, and we call these species zwitterionic silenes. The geometries of neutral zwitterionic silenes are similar to those of anionic species, such as 2-silenolates. A plot of $r_{\mathrm{Si=C}}$ versus $q(\mathrm{Si})$ of the various Si=C bonded compounds reveals two linear parts separated by a breakpoint at which the Si pyramidalization also sets in. A connection between CGMT theory and that of reversed polarization was found.

Silenes influenced by reversed polarization are less prone to dimerize than the parent silene, and dimerization energies of fully zwitterionic silenes can be as low as 14 kcal mol^{-1}. There is no clear preference for head-to-tail or head-to-head dimerization for either type of silene. However, a possible reaction channel for the reverse-polarized 2,2-dialkoxy-substituted silenes is rearrangement to their 1,1-disubstituted isomers, since the energy gain in this process is large ($\approx$60 kcal mol^{-1} at the B3LYP/6-31 + G(d) level). These rearranged silenes would dimerize easily, since some further 100 kcal mol^{-1} is gained in this process. Inductively electron-donating substituents at Si lower the dimerization energy, whereas the opposite is true for inductively withdrawing substituents, in a similar manner as previously concluded by Gusel'nikov.[47]

The charge at the Si atom of zwitterionic silenes resembles that of silyl anions, and the influence of Si substituents on the properties of silyl anions and zwitterionic silenes is similar. Inductively electron-withdrawing substituents at Si raise their E_{inv} values, and silenes with inversion barriers as high as 35 kcal mol^{-1} are found computationally. The high E_{inv} in zwitterionic silenes enables computational design of silenes with chiral Si atoms. It now needs to be probed if these chiral silenes can be realized. Together with our recent finding that reactions of dienes with zwitterionic silenes proceed more selectively in a [4+2] manner than with naturally polarized silenes, we hope that these findings could render silenes of general interest to synthetic organic chemistry.

Acknowledgement

The author is grateful to the Wenner–Gren Foundations and the Swedish Research Council (VR) for financial support, as well as to the Nationellt Superdatorcentrum (NSC) in Linköping, Sweden, for generous allotments of computer time.

---

[1] For reviews on silenes, see a) A. G. Brook, M. Brook, *Adv. Organomet. Chem.* **1996**, *39*, 71; b) T. Müller, W. Ziche, N. Auner in *The Chemistry of Organic Silicon Compounds, Vol. 2* (Eds.: Z. Rappoport, Y. Apeloig), Wiley Interscience, New York, **1998**, p. 857.

[2] Y. Apeloig, M. Karni, *J. Am. Chem. Soc.* **1984**, *106*, 6676.

[3] a) A. G. Brook, F. Abdesaken, B. Gutekunst, G. Gutekunst, R. K. Kallury, *J. Chem. Soc. Chem. Commun.* **1981**, 191; b) A. G. Brook, S. C. Nyburg, F. Abdesaken, B. Gutekunst, G. Gutekunst, R. K. M. R. Kallury, Y. C. Poon, Y.-M. Chang, W. Wong-Ng, *J. Am. Chem. Soc.* **1982**, *104*, 5667.

[4] a) W. J. Leigh, R. Boukherroub, C. Kerst, *J. Am. Chem. Soc.* **1998**, *120*, 9504; b) W. J. Leigh, C. Kerst, R. Boukherroub, T. L. Morkin, S. I. Jenkins, K. Sung, T. T. Tidwell, *J. Am. Chem. Soc.* **1999**, *121*, 4744; c) T. L. Morkin, W. J. Leigh, *Acc. Chem. Res.* **2001**, *34*, 129.

[5] a) K. Sakamoto, J. Ogasawara, H. Sakurai, M. Kira, *J. Am. Chem. Soc.* **1997**, *119*, 3405; b) T. Veszprémi, M. Takahashi, J. Ogasawara, K. Sakamoto, M. Kira, *J. Am. Chem. Soc.* **1998**, *120*, 2408; c) T. Veszprémi, M. Takahashi, B. Hajgató, J. Ogasawara, K. Sakamoto, M. Kira, *J. Phys. Chem. A.* **1998**, *102*, 10530; d) M. Takahashi, K. Sakamoto, M. Kira, *Int. J. Quant. Chem.* **2001**, *84*, 198; e) K. Sakamoto, J. Ogasawara, Y. Kon, T. Sunagawa, C. Kabuto, M. Kira, *Angew. Chem.* **2002**, *114*, 1460; *Angew Chem. Int. Ed. Engl.* **2002**, *41*, 1402.

[6] a) G. E. Miracle, J. L. Ball, D. R. Powell, R. West, *J. Am. Chem. Soc.* **1993**, *115*, 11598; b) M. Trommer, G. E. Miracle, B. E. Eichler, D. R. Powell, R. West, *Organometallics* **1997**, *16*, 5737.

[7] I. El-Sayed, T. Guliashvili, R. Hazell, A. Gogoll, H. Ottosson, *Org. Lett.* **2002**, *4*, 1915.

[8] a) J. Ohshita, Y. Masaoka, S. Masaoka, M. Ishikawa, A. Tachibana, T. Yano, T. Yamabe, *J. Organomet. Chem.* **1994**, *473*, 15; b) J. Ohshita, S. Masaoka, Y. Masaoka, H. Hasebe, M. Ishikawa, A. Tachibana, T. Yano, T. Yamabe, *Organometallics* **1996**, *15*, 3136; c) J. Ohshita, S. Masaoka, M. Ishikawa, *Organometallics* **1996**, *15*, 2198; d) J. Ohshita, S. Masaoka, Y. Morimoto, M. Sano, M. Ishikawa, *Organometallics* **1997**, *16*, 1123; e) J. Ohshita, H. Sakurai, Y. Tokunaga, A. Kunai, *Organometallics* **1999**, *18*, 4545; f) J. Ohshita, H. Sakurai, S. Masaoka, M. Tamai, A. Kunai, M. Ishikawa, *J. Organomet. Chem.* **2001**, *633*, 131; g) J. Ohshita, M. Tamai, H. Sakurai, A. Kunai, *Organometallics* **2001**, *20*, 1065.

[9] T. Guliashvili, I. El-Sayed, A. Fischer, H. Ottosson, *Angew. Chem.* **2003**, *115*, 1678; *Angew. Chem. Int. Ed.* **2003**, *42*, 1640.

[10] G. Maier, H. P. Reisenauer, H. Egenolf, *Organometallics* **1999**, *18*, 2155.

[11] W. M. Boesveld, B. Gehrhus, P. B. Hitchcock, M. F. Lappert, P. von R. Schleyer, *J. Chem. Soc. Chem. Commun.* **1999**, 755.

[12] a) S. Bailleux, M. Bogey, J. Breidung, H. Bürger, R. Fajgar, Y. Liu, J. Pola, M. Senzlober, W. Thiel, *Angew. Chem.* **1996**, *108*, 2683; *Angew. Chem. Int. Ed. Engl.* **1996**, *35*, 2513; b) S. Bailleux, M. Bogey, J. Demaison, H. Bürger, M. Senzlober, J. Breidung, W. Thiel, R. Fajgar, J. Pola, *J. Chem. Phys.* **1997**, *24*, 10016.

[13] H. S. Gutowsky, J. Chen, P. J. Hajduk, J. D. Keen, C. Chuang, T. Emilsson, *J. Am. Chem. Soc.* **1991**, *113*, 4747.

[14] Y. Apeloig, M. Bendikov, M. Yuzefovich, M. Nakash, D. Bravo-Zhivotovskii, *J. Am. Chem. Soc.* **1996**, *118*, 12228.

[15] N. Wiberg, G. Wagner, G. Müller, *Angew. Chem.* **1985**, *24*, 229; *Angew. Chem. Int. Ed. Engl.* **1985**, *24*, 229.

[16] a) E. A. Carter, W. A. Goddard III, *J. Phys. Chem.* **1986**, *90*, 998; b) E. A. Carter, W. A. Goddard III, *J. Chem. Phys.* **1988**, *88*, 1752.

[17] a) G. Trinquier, J.-P. Malrieu, *J. Am. Chem. Soc.* **1987**, *109*, 5303; b) J.-P. Malrieu, G. Trinquier, *J. Am. Chem. Soc.* **1989**, *111*, 5916; c) G. Trinquier, J.-P. Malrieu in *Supp. A: The Chemistry of Double-Bonded Functional Groups, Vol. 2, Part 1* (Ed.: S. Patai), Wiley, Chichester, **1989**, p. 1.

[18] For a review on connections of the CGMT theory to experimental results, see M. Driess, H. Grützmacher, *Angew. Chem.* **1996**, *108*, 900; *Angew. Chem. Int. Ed. Engl.* **1996**, *35*, 828.

[19] M. Karni, Y. Apeloig, *J. Am. Chem. Soc.* **1990**, *112*, 8589.

[20] W.-C. Chen, M.-D. Su, S.-Y. Chu, *Organometallics* **2001**, *20*, 564.

[21] H. Jacobsen, T. Ziegler, *J. Am. Chem. Soc.* **1994**, *116*, 3667.

[22] C. Liang, L. C. Allen, *J. Am. Chem. Soc.* **1990**, *112*, 1039.

[23] K. Aarset, A. G. Császár, E. L. Sibert III, W. D. Allen, H. F. Schaefer III, W. Klopper, J. Noga, *J. Chem. Phys.* **2000**, *112*, 4053.

[24] A. D. Becke, *J. Chem. Phys.* **1993**, *98*, 5648.

[25] P. S. Hariharan, J. A. Pople, *Theor. Chim. Acta* **1973**, *28*, 213.

[26] A. E. Reed, L. A. Curtiss, F. Weinhold, *Chem. Rev.* **1988**, *88*, 899.

[27] A. D. McLean, G. S. Chandler, *J. Chem. Phys.* **1980**, *72*, 5639.

[28] R. Krishnan, J. S. Binkley, R. Seeger, J. A. Pople, *J. Chem. Phys.* **1980**, *72*, 650.

[29] a) S. Miertus, E. Scrocco, J. Tomasi, *Chem. Phys.* **1981**, *55*, 117; b) S. Miertus, J. Tomasi, *Chem. Phys.* **1982**, *65*, 239; c) M. Cossi, V. Barone, R. Cammi, J. Tomasi, *Chem. Phys. Lett.* **1996**, *255*, 327.

[30] a) D. Cremer, E. Kraka, *Croat. Chem. Acta* **1984**, *57*, 1259; b) D. Cremer, E. Kraka, *Angew. Chem.* **1984**, *96*, 612; *Angew. Chem. Int. Ed. Engl.* **1984**, *23*, 627.

[31] Gaussian 98, Revision A.9, M. J. Frisch, G. W. Trucks, H. B. Schlegel, G. E. Scuseria, M. A. Robb, J. R. Cheeseman, V. G. Zakrzewski, J. A. Montgomery, Jr., R. E. Stratmann, J. C. Burant, S. Dapprich, J. M. Millam, A. D. Daniels, K. N. Kudin, M. C. Strain, O. Farkas, J. Tomasi, V. Barone, M. Cossi, R. Cammi, B. Mennucci, C. Pomelli, C. Adamo, S. Clifford, J. Ochterski, G. A. Petersson, P. Y. Ayala, Q. Cui, K. Morokuma, D. K. Malick, A. D. Rabuck, K. Raghavachari, J. B. Foresman, J. Cioslowski, J. V. Ortiz, A. G. Baboul, B. B. Stefanov, G. Liu, A. Liashenko, P. Piskorz, I. Komaromi, R. Gomperts, R. L. Martin, D. J. Fox, T. Keith, M. A. Al-Laham, C. Y. Peng, A. Nanayakkara, M. Challacombe, P. M. W. Gill, B. Johnson, W. Chen, M. W. Wong, J. L. Andres, C. Gonzalez, M. Head-Gordon, E. S. Replogle, J. A. Pople, Gaussian, Inc., Pittsburgh PA, **1998**.

[32] AIM2000, Version 1.0, F. Biegler-König, D. Bayles, J. Schönbohm, University of Applied Sciences, Bielefeld, Germany, **2000**.

[33] T. J. Lee, P. R. Taylor, *Int. J. Quant. Chem.* **1989**, *S23*, 199.

[34] R. Beccera, R. Walsh in *The Chemistry of Organic Silicon Compounds, Vol. 2* (Eds.: Z. Rappoport, Y. Apeloig), Wiley, Chichester, UK, **1998**, p. 153.

[35] a) R. L. Pruett, J. T. Barr, K. E. Rapp, C. T. Bahner, J. D. Gibson, R. H. Lafferty, *J. Am. Chem. Soc.* **1950**, *72*, 3646; b) H. Kropf, E. Schaumann, *Houben-Weyl: Metoden der Organischen Chemie*, George Thieme Verlag, Stuttgart, **1993**, *E15*, 2899.

[36] R. S. Grev, H. F. Schaefer III, K. M. Baines, *J. Am. Chem. Soc.*, **1990**, *112*, 9458.

[37] V. Jonas, G. Frenking, M. T. Reetz, *J. Am. Chem. Soc.* **1994**, *116*, 8741.

[38] M. W. Schmidt, M. S. Gordon, M. Dupuis, *J. Am. Chem. Soc.* **1985**, *107*, 2585.

[39] R. Walsh, *Acc. Chem. Res.* **1981**, *14*, 246.

[40] W. J. Pietro, W. J. Hehre, *J. Am. Chem. Soc.* **1982**, *104*, 4329.

[41] M. Ichinohe, T. Tanaka, A. Sekiguchi, A. *Chem. Lett.* **2001**, 1074.

[42] M. Bendikov, S. R. Quadt, O. Rabin, Y. Apeloig, *Organometallics*, **2002**, *21*, 3930.

[43] D. Bergmann, J. Hinze in *Structure and Bonding: Electronegativity* (Eds.: K. D. Sen, C. K. Jørgensen), Springer-Verlag, Berlin, **1987**, p. 145.

[44] The group electronegativities of CH_3 and CHO in the Pauling scale are 2.30 and 3.18 according to ref. [43].

[45] A value of 110.6 kcal mol^{-1} was used for $E_{\sigma+\pi}$ derived from the dissociation of $H_2Si{=}CH_2$ into the electronic ground states of H_2Si (1^1A_1) and H_2C (1^3B_1) at the (U)B3LYP/6-31+G(d) level. The occupations of the 2pπ(C) and 3pπ(Si) AOs in the carbenes and silylenes were obtained from natural population analysis by using the B3LYP/6-31+G(d) densities.

[46] J. C. Poutsma, J. A. Paulino, R. R. Squires, *J. Phys. Chem. A*, **1997**, *101*, 5327.

[47] L. A. Gusel'nikov, V. G. Avakyan, S. L. Guselnikov, *J. Am. Chem. Soc.* **2002**, *124*, 662.

[48] a) A. G. Brook, K. D. Safa, P. D. Lickiss, K. M. Baines, *J. Am. Chem. Soc.* **1985**, *107*, 4338; b) K. M. Baines, A. G. Brook, R. R. Ford, P. D. Lickiss, A. K. Saxena, W. J. Chatterton, J. F. Sawyer, B. A. Behnam, *Organometallics* **1989**, *8*, 693; c) P. Lassacher, A. G. Brook, A. J. Lough, *Organometallics* **1995**, *14*, 4359.

[49] a) A. C. Hopkinson, C. F. Rodriques, M. H. Lien, *Can. J. Chem.* **1990**, *68*, 1309; b) J. R. Damewood, Jr., C. M. Hadad, *J. Phys. Chem.* **1988**, *92*, 33.

[50] a) B. M. Gimarc, *Molecular Structure and Bonding*, Academic Press, New York, **1980**; b) T. A. Albright, J. K. Burdett, M.-H. Whangbo,. *Orbital Interactions in Chemistry*, Wiley Interscience, New York, **1985**.

[51] The norm of the amplitude of single excitations in the CCSD/6-311+G(d)//B3LYP/6-31+G(d) wave function is 0.015 (i.e., lower than the value of 0.02 used as a threshold in ref. [33] for an indicator of multireference character).

[52] a) L. H. Sommer, R. Mason, *J. Am. Chem. Soc.* **1965**, *87*, 1619; b) C. Eaborn, R. A. Jackson, M. T. Rahman, *J. Organomet. Chem.* **1972**, *34*, 7; c) E. Colomer, R. Corriu, *J. Chem. Soc. Chem. Commun.* **1976**, 176; d) E. Colomer, R. J. P. Corriu, *J. Organomet. Chem.* **1977**, *133*, 159; e) M. Omote, T. Tokita, Y. Shimizu, I. Imae, E. Shirikawa, Y. Kawakami, *J. Organomet. Chem.* **2000**, *611*, 20; f) C. Strohmann, J. Hörnig, D. Auer, *J. Chem. Soc. Chem. Commun.* **2002**, 766.

Received: November 19, 2002
Revised: April 4, 2003 [F4583]